Generation of KI mice with neo disrupted mTOR

mTOR sequence obtained from GenBank (AC108508) revealed that it has 58 exons and 57 introns. An 8.6-kb BamHI genomic fragment encompassing exons 9–17 of the mTOR gene was isolated from a BAC library (129 SVJ mouse, Genome Systems, INC. St. Louis, MO) and sub-cloned into pBluescript II KS vector (Stratagene). Exon12 of mTOR was replaced with BALB/c sequences, including one EcoRI site**.** The neo gene under the phosphoglycerate kinase 1 promoter (pGKneo) was employed as a positive selectable marker; a pGK-thymidine kinase cassette was used as a negative selectable marker (22). A LoxP site was inserted before exon 12 and a frt-loxP-pGKEM7-neo-frt-loxP cassette was inserted into intron 12 (Fig. S1A). All vectors and cloning steps were confirmed by sequencing. Electroporation and selection were performed using the CJ7 ES cell line as described (22). DNAs derived by G418/FIAU resistant ES clones were screened using 5' and 3' probes external to the targeting vector sequence. Five independent targeted ES cell clones for the mTOR gene injected into C57BL/6 blastocysts generated chimeras that transmitted the mutated allele to the progeny (23). Knock-in mice containing the neo gene were bred to β-actin cre mice (36). The resultant progeny (KI^{neo-}) deleted neo ubiquitously, but retained exon 12 and the 628C allele of mTOR. Mice were bred in specific, pathogen-free and conventional facilities (LCBG-009) with food and water *ad libitum*. All animals were treated in accordance with the guidelines provided by the Animal Care and Use Committee of the National Cancer Institute.

Genotyping

KI offspring carrying neo-mTOR were identified by PCR of tail DNA using forward (5′-CCTTGGCAGCTTTGAATTTGAAG-3′) and reverse (5′-CAGAGACAGGAGACGAAGAACAGG-3′) primers. 239 and 273 bp fragments were amplified from the WT and KI, respectively. Genotyping was also confirmed by sequencing.

Immunizations and measurements of antibody titers

Groups (n = 5 ea) of WT, KI and KI^{neo-} mice, 9 weeks of age, were immunized with either NP-LPS (100ug) or NP-CGG (100ug) in 100 µl PBS with 25 µg of rehydagel (Reheis). Vehicle controls were in 100 µl PBS with 25 µg of rehydragel . Sera were collected at day 7 for NP-LPS and either day 14 or 21 for NP-CGG, and both total antibody concentrations and NP-specific titers were measured by ELISA (total IgM and IgG: Immnology Consultants Laboratory, Inc.; NP-specific antibodies: SBP Clonotyping™ System/AP & Southern Biotech; NP-BSA for coating plates: Biosearch Technologies, Inc).

Northern blot and real-time RT-PCR

Total RNA was isolated from different tissues and cells by TRIzol Reagent (Invitrogen) and analyzed by northern blot. mTOR transcripts were detected by using mouse specific mTOR probes (5′ probe spanning exons 6–9; 3′ probe spanning exons 40–46) and a neomycin DNA probe. cDNAs were made by TaqMan Reverse Transcription Reagents (Applied Biosystems: N808-0234), real-time PCR was performed using SYBR Green PCR Master Mix (Part No: 4309155, ABI 7500) with the following primers: forward primer: 5'-CCCTTCGTGCCTGTCTGATT-3'; reverse primer: 5'-CTCGATTCATACCCTTCTCTTTGG-3'.

Preparation of MEFs and primary fibroblast cells
MEFs were prepared from day 13.5 embryos derived from crosses between neo-mTOR heterozygous mice. Each embryo was carefully removed from the embryonic sac, minced, dispersed in 0.05% trypsin-EDTA solution, and incubated for 30 minutes at 4°C. A small piece from each embryo was used for genotyping. The primary fibroblast cells were prepared from tail tips (<1cm); tips were digested in 5 ml of collagenase (8 mg/ml) at 37°C for 30 minutes. Cells (MEFs and fibroblasts) were plated in 75 cm plates containing DMEM plus 10% FBS, incubated at 37°C until confluent, and frozen down or replated. Fibroblast cells were not passaged more than 5×.

Preparation of lymphocytes, macrophage, and neutrophils from mice
Cells were separated from different organs or tissues, and red blood cells (RBC) were removed with ACK lysis buffer. Total T cells, CD4+ T cells, CD19+ and B220+ B cells, and CD11b+ macrophages were purified with MACS kits (Pan T cell, catalog no.: 130-049-861; CD4, catalog no. 130-091-041;CD19 catalog no: 130-052-201; CD11b catalog no: 130-049-601). Total lymphocytes or B220+ cells were stimulated with 50 μg/ml of LPS (Sigma) for 48 hours prior to the collection of cell lysates. For inhibitor studies, cells were pretreated with 20 μM of DNA-PKcs inhibitor NU7026 (Tocris Bioscience) for 2 hours prior to LPS activation. S1P chemotaxis was performed using Cytoselect plates/reagents (Cell Biolabs, Inc.); purified cells resuspended in serum-free media were allowed to migrate toward the chemokine for 3 h. Mouse bone marrow neutrophils were isolated as described and resuspended in HBSS for chemotaxis measurements (25). Purity of the cell population was assessed by staining with Kimura stain and was between 70–80%. The EZ-Taxiscan chamber (Effector Cell Institute, Japan) was used to assess chemotaxis according to manufacturer's protocols (26). Cells were plated on untreated glass, allowed to migrate towards 100 μM fMLP (Sigma), and imaged every 20 secs for 90 min. Migrations paths were obtained using MatLab (Fig. S10, Video 1).

Cell growth analyses
MEF cells were cultured in DMEM containing 10% FBS and penicillin-streptomycin. The cells were seeded in 12-well plates with 10^5 cells/well and counted every day for 4 days with Trypan blue staining. Cells were isolated from thymus, spleen, bone marrow, or lymph node, and RBC were removed with ACK buffer. T cells, $B220^+$ B cells, and $CD43^-$ B cells were purified using MACS kits. Cells were cultured in RPMI 1640 medium containing 10% FBS, 50 μM 2-mercaptoethanol, 2 mM L-glutamine, and penicillin-streptomycin starting with $1–2 \times 10^5$ cells/well in 96-well plates with flat bottoms. The B cells were stimulated for 4 days with either 3μg/ml LPS (Sigma L2880-25mg), α-mouse-CD40 (BD Biosciences,553687) plus 500U/ml mouse IL4 (PeproTech, Inc., 214-14) or α-mouse IgM (Jackson Immuno-Research Labs,115-006-020) plus 500U/ml mouse IL4 in a final volume of 100μl/well culture medium. The T cells were stimulated with 1 μg/ml α-mouse CD3ε antibody coated plates plus 5 μg/ml α-mouse CD28 antibody. Purified splenocytes were activated with the indicated concentrations of α-CD3ε + α-CD28 (5μg/ml) for 72h and then pulsed with ^{3}[H]-deoxythymidine for 8 h and analyzed for thymidine incorporation to assess T-cell proliferation. Comparisons with WST-1 viability reagents (Roche,1644807) yielded similar results, and as such this assay was used to compare cell proliferation/viability of B cells stimulated with different ligands.

Rapamycin treatment of the myeloma cell line
Rapamycin (sirolimus) was provided by the Drug Synthesis and Chemistry Branch (DSCB), Developmental Therapeutics Program(DTP), Division of Cancer Treatment and Diagnosis (DCTD), National Cancer Institute (NCI), National Institutes of Health (NIH). Rapamcyin was dissolved in dimethylsulfoxide (DMSO; Sigma) at a concentration of 10mM and stored at −20°C. L363 myeloma cells were treated for 24 hours with 10nM rapamycin with $\leq$0.2 %DMSO.

Western blot analysis
Protein extracts from tissues and cell cultures were prepared with lysis buffer (50mM Tris-HCl, pH 7.4, 150mM NaCl, 1% NP-40, 1mM EDTA, 20mM Beta Glycerol Phosphate, Roche cock-tail proteinase inhibitors, and phosphatase cock-tail A and B inhibitors (Santa Cruz). 20µg of protein lysate was used for Western blot analysis. All antibodies, including the C-terminal antibody for mTOR used in all of the signaling experiments, came from Cell Signaling, except for the following: mTOR N-terminal (Calbiochem), α-Rictor (Novus), Deptor (SDI), ERK and pERK (Chemicon International), $S1P_1$ (ProSci), SIP3 and KLF2 (Life Span).

Cellular localization assay
Cells grown on coverslips were fixed with 3.5% paraformaldehyde, permeabilized with 0.5% Triton X100, blocked with 10% FBS, and blotted with anti-mTOR antibody. Stained cells were mounted with Vectashield/DAPI, and examined using fluorescence microscopy (Fig. S2B).

Flow cytometry analysis
All unlabelled antibodies, phycoerythrin (PE), fluorescein isothiocyanate (FITC), APC, or PerCP-conjugated were purchased from BD Pharmingen or eBioscience. Cells were separated from different organs or tissues, and red blood cells removed using ACK lysis buffer. Stained cells were resuspended in FACS buffer (PBS with 0.5% BSA) to a final concentration of 10^7 cell/ml. 100 µl of cells, blocked with Fc blocker (anti-CD16/32) for 15 minutes (min) at 4°C, incubated with single antibodies or an antibody cocktail at 4°C for 30 min, and washed twice with FACS buffer. Cells were fixed with 400 µl FACS buffer containing 1% of paraformaldehyde. Cells (for phospho-Akt–specific flow cytometry) were first fixed in 2% paraformaldehyde for 10 min at 37°C, washed twice with FACS buffer, blocked with Fc blocker for 15 min at 4°C, and then stained with different antibodies for 30 min at 4°C. To permeabilize, cells were resuspended in 100 µl of FACS buffer, 90 µl of ice cold MeOH added slowly, then vortexed briefly, and incubated for 30 min at 4°C. Cells were washed twice, incubated for 15 min at room temperature (RT), and stained with anti–phospho-Akt antibody (Catalog No 4058, Cell Signaling) for 1 hour at RT. Cells were washed twice, resuspended in 100 ul of Alexa Fluor 488-conjugated secondary antibody solution (Molecular Probes, catalog No A21206) for 30 minutes at RT. Cells were washed twice. Stained cell populations and cell sizes were obtained with FACSCalibur and analyzed using Flowjo8.7.

Detecting NF-κB activation and IκBα degradation
Nuclear extracts were prepared from LPS (50 ug/ml for 24 hours) stimulated bone marrow (BM) cells using Active Motif kits (40010,40410); protein concentrations were determined using Pierce protein assay reagents (1861426). ELISA-based kits (TransAM kit, Active Motif) were used to detect/quantify NF-κB p50, p65 and p52 activation. Cells were stimulated with different

concentrations of LPS and protein lysates prepared with RIPA buffer containing proteinase inhibitors. IκBα degradation was tested by western blot with anti-IκBα antibody (Santa Cruz, SC371).

Figure S1. Generation of mice with disrupted mTOR expression
(A) Diagram of the knock-in construct used to generate mice with a 628C allele (exon 12) of mTOR. This resulted in a functional knockdown of mTOR expression by neo interference. A pGKneobpA cassette flanked by LoxP sites was inserted into intron 12; a LoxP site was also inserted before exon12. (B) Northern blot analysis of total RNA extracted from brains of either wild-type (WT), heterozygous (HET) for the knock-in with neo, or homozygous for the knock-in (KI) with neo, hybridized with either a 5′ probe (exon 6–9), or a neo probe. Transcripts detected by the probes are: 9.2 kb (full-length mTOR), 4.3 kb (fusion: mTOR exons 1–12 plus neo), and 1.3 kb (neo only). The insertion of the neo gene causes a splice into the neo gene and a premature termination of the transcript since the 5' probe detects an mRNA message containing both the upstream part of mTOR as well as the neo gene (4.3 Kb band). In addition, we also detect a neo specific transcript that due to the small size does not appear to include any additional downstream sequence of mTOR.

Figure S2. Reduced expression of mTOR in homozygous KI mice
(A) Western blot analysis of mTOR protein expression in different tissues. (B) Staining with mTOR antibody (red) revealed some overlap with DAPI (blue) stained nuclei, but was localized predominantly in the cytoplasm of fibroblasts derived from WT, HET, or KI mice. Cells were examined at 25°C with a Zeiss LSM 510 NLO confocal system (Carl Zeiss Inc, Thornwood, NY, USA) with an Axiovert 200M inverted microscope and operating with a 2-photon laser tuned to 750 nm, 25 mW argon laser tuned to 488 nm, and 1 mW HeNe laser tuned to 543 nm. Cells were imaged with a 63× 1.4 NA Zeiss Plan-Apochromat oil immersion objective. Digital images (512 × 512 pixels, 8 bit) were collected using the Zeiss AIM software with a scan zoom from 2 to 4 and a multi-track configuration where the Texas Red, and DAPI signals were collected sequentially with a BP 565–615 nm filter, and BP 390–465 nm filter after excitation with 543 nm and 750 nm laser lines, respectively.

Figure S3. TORC1 and TORC2 kinase activity in fibroblasts/T cells of KI mice.
(A) Protein expression of mTOR, RAPTOR and RICTOR in skin fibroblasts of WT, HET, and KI mice. (B) Western blot analysis of protein extracts from fibroblasts for mTOR and its TORC1 targets. In KI fibroblasts, lower mTOR levels resulted in less phosphorylation of p70S6K on Thr389 and pS6 on Ser240/244. (C) Dose response of p-p70S6K^{Thr389} in fibroblasts after insulin treatment (1–100 nM for 10 min). KI fibroblasts responded in a dose-dependent fashion to insulin stimulation with increasing amounts of p-p70S6K^{Thr389}, albeit with lower levels of phosphorylation than those of WT mice. (D) Western blot analysis of protein extracts for the TORC2 target, AKT. There was a modest decrease in pAKT^{Ser473} in KI fibroblasts. (E) MEF cells from WT and KI mice had similar AKT and pAKT levels following stimulation with either 10 or 100 nM of insulin for 15 min. (F) Thymic T cells from KI mice had lower levels of pAKT^{Ser473} after 30 min. stimulation with α-CD3ε/CD28. In contrast, pERK levels in the KI thymus were equivalent to those of the WT. (G) DEPTOR (a protein that associates with both TORC1 and TORC2) levels in KI mice are slightly increased relative to those in WT mice. (H) Viability/growth curves for mouse embryo fibroblasts (MEF) were determined using WST-1 (left) or cell counting by trypan blue (right). MEFs from KI mice had lower viability/proliferation rates. Data are presented as mean±SEM; *, significance $P<0.01$. Each group had 6 samples.

Figure S4. T-cell populations in thymus, spleen and lymph nodes
Average cell numbers (A–C) of CD4 and CD8 T cells in thymi, spleens, and lymph nodes of WT and KI mice (N = 5). The proportions of CD4 and CD8 SP T cells were increased in the thymus (A) and spleen (B) of KI mice. In contrast, $CD4^+$ T cells were slightly lower in the KI lymph nodes (C) and $CD8^+$ T cells were unchanged. (D–F) Relative size distributions (forward scatter, FSC-H) of $CD4^+$ and CD8 T^+ cells in thymi, spleens, and lymph nodes of WT and KI mice. Except for CD4/CD8 double positive cells in the thymus, all other T-cell sizes were smaller in the KI mice relative to the WT.

Figure S5. T-cell migration and CD4, CD8 cell populations in thymus, spleen and lymph nodes
(A) Thymic T cells isolated from KI mice did not migrate as well to TECK and SDF. The majority of CD4 and CD8 SP cells in KI (blue) (B) spleens and (C) lymph nodes were $CD44^{lo}$ and $CD62L^{hi}$ suggesting a naïve phenotype. (D) S1P1 (EDG1) receptor expression was slightly lower in $CD4^+$ and $CD8^+$ splenic cells. (E) Single positive CD4 and CD8 thymic T cells from KI versus WT showed few differences in CD5, CD24, or TcRβ expression.

Figure S6. T-cell proliferation and survival
(A) Differences in WST-1 (viability) staining of splenic T cells stimulated with anti-CD3e plus anti-CD28 from WT vs KI mice were similar to proliferation data measured by tritiated thymindine incorporation (see Fig. 3A). Data are presented as mean±SEM; *, significance $P<0.001$. Each group had 5 samples. (B) CD4 T cells from KI spleens cultured in the presence or absence of IL7, did not undergo apoptosis as readily as WT cells, as measured by staining positive for both Annexin V and 7-AAD. A representative plot is shown from one of 3 independent experiments examining cells from 1–2 mice each. Similar results were seen for CD8 T cells (data not shown.)

Figure S7. NF-κB activity/IkB degradation and PLCγ2 levels in WT and KI mice.
(A–D) NFκB activation (p50, p65 and p52) as measured by ELISA in nuclear extracts of LPS stimulated $B220^+$ cells isolated from the bone marrow were not altered in the KI mice; WT and KI values were equivalent for canonical pathway members p50 (A) and p65 (B), and for the non-canonical pathway member, p52 (C). (D) IκB degradation in LPS stimulated B220+ bone marrow cells also did not show differences between WT and KI mice. (E) PLCγ2 protein levels in B220+ splenic lymphocytes from WT and KI mice.

Figure S8. mTOR expression alters B-cell differentiation in the spleen
Splenic $B220^+$ cells were also stained with IgM and IgD antibodies and stages of B cells were identified by the following cell surface markers: T1: transitional B cells ($B220^+IgD^{low}IgM^{hi}CD23^-$). The average percentages of mature B cells were higher in KI mice; however, average percentages of T1 (A), marginal zone (MZ: $B220^+IgD^{low}IgM^{hi}CD23^-CD21^{hi}$) (A,B) and follicular (B) B cells were reduced in KI mice.

Figure S9
(A–C) WST-1 viability staining for splenic $CD43^-$ resting B lymphocytes of WT and KI mice after treatment with either 3μg/ml of α-IgM antibody and 500U/ml of IL4 (A), or with 3μg/ml of α-CD40 antibody and 500U/ml of IL4 (B), or with 3μg/ml of LPS (C). Data are presented as

mean±SEM; *, significance $p<0.001$. N = 6 for each group. One of three similar experiments using WT and KI mice is shown.

Figure S10. Neutrophils and monocytes
(A) Populations of GR1/CD11b precursor cells from the BM were not different between WT and KI mice, yet (B) the percentages of Gr1+ and Mac-1+ splenic cells were reduced in the KI mice. (C) Activity/migration plots of KI neutrophils (1.9 ± 1.0 μm/min) isolated from the BM revealed that neutrophils expressing low mTOR levels (Western blot) behave similarly ($p >0.05$) to neutrophils isolated from WT animals (2.1 ± 1.3 μm/min) (see Video 1). Cells were set up on untreated glass and exposed to a stable, linear gradient of fMLP established by adding 100 μM in the bottom well. Images were acquired every 20s for 90 min at room temperature. Individual cell speed and chemotaxis indices were assessed using Matlab.

Figure S11. Neo-less mTOR 628C KI mice (KI^{neo-}) are relatively normal (equal to WT) except for p4EBP1
(A) mTOR protein levels in spleens of KI^{neo-} mice were equivalent to WT (N = 3 ea). (B) Body weights and (C) cell sizes as well as (D) total numbers of splenocytes were also equivalent in WT and KI^{neo-} mice. (E, F) Percentages of $B220^+$ splenic lymphocytes in KI^{neo-} mice were equivalent to those in WT mice. (G) $CD4^+$ and $CD8^+$ T-cell populations in the thymus and spleen were also normal in the KI^{neo-} mice. (H) Viability/proliferation of $B220^+$ cells in the spleens of KI^{neo-} mice were similar to WT cells. (I) TORC1/TORC2 targets in MEF cells stimulated with 100nM insulin (0,5, 10 min) were similar in WT and KI^{neo-} mice. (J) p-AKT^{Ser473} levels in splenic B220+ cells stimulated with LPS were the same in WT and KI^{neo-} mice (2 mice each). (K) Phosphorylation of 4EBP1 on Thr37/46 was decreased in the BM of neoless KI mice carrying the 628C allele relative to WT (2 mice each).

Figure S1

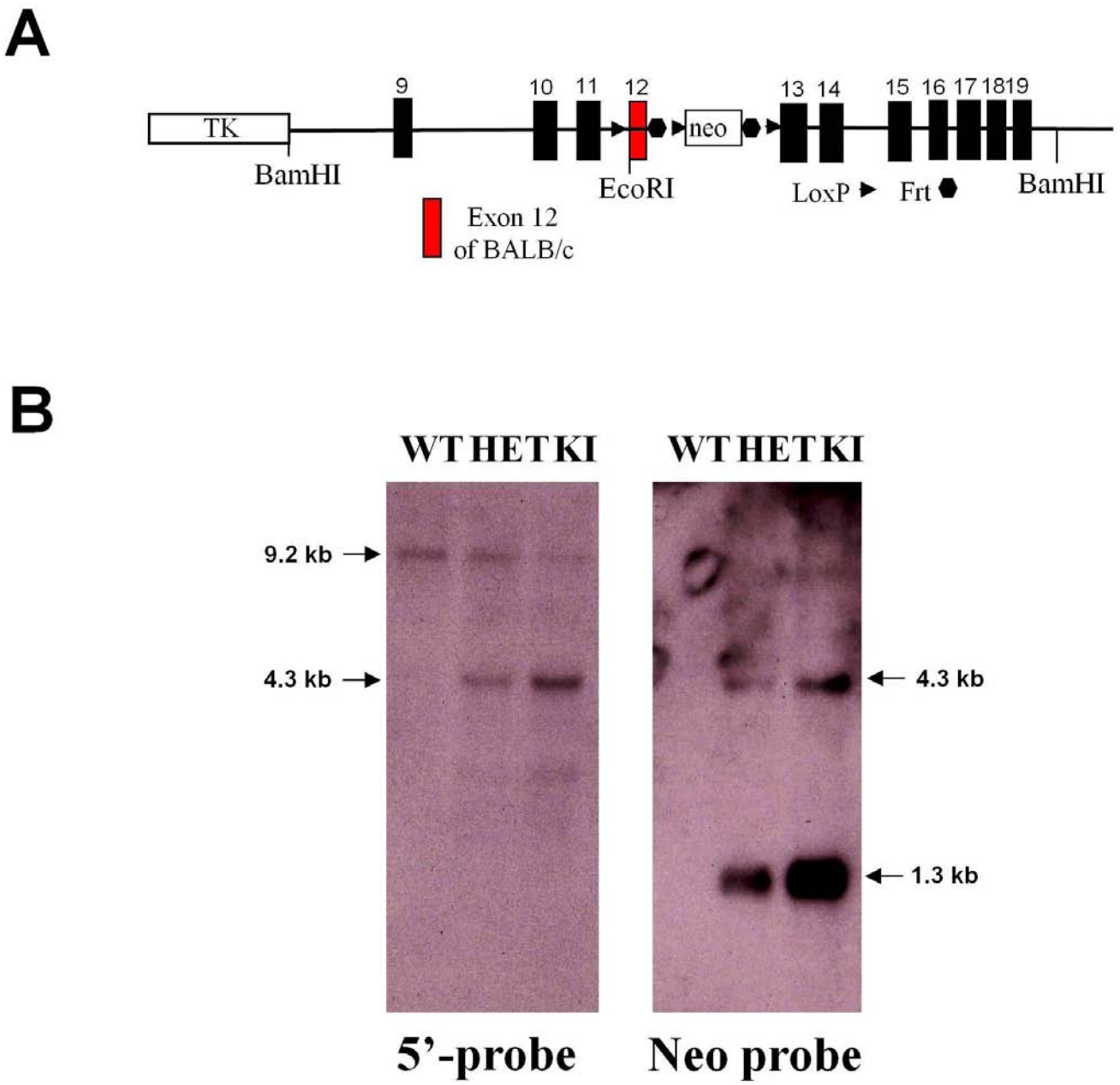
A
9
10
11
12
13
14
15
16
17
18
19
TK
neo
BamHI
EcoRI
LoxP
Frt
BamHI
Exon 12
of BALB/c
B
WT HET KI
WT HET KI
9.2 kb
4.3 kb
4.3 kb
1.3 kb
5'-probe
Neo probe

Figure S2

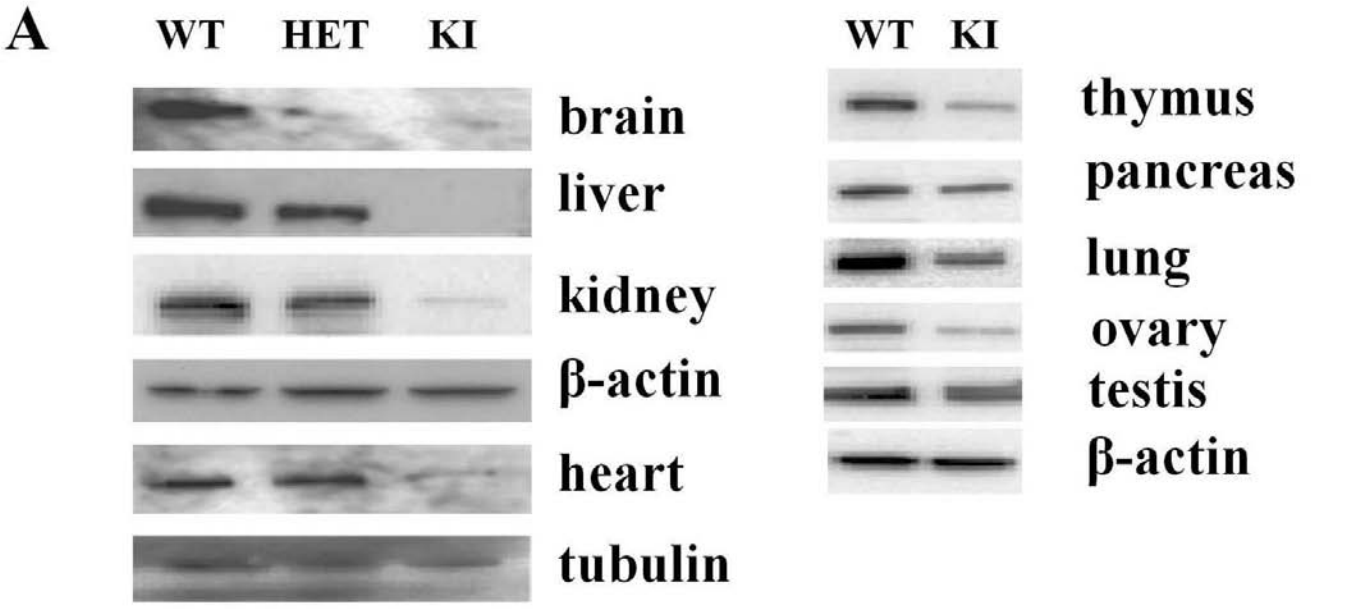
A
WT
HET
KI
brain
liver
kidney
β-actin
heart
tubulin
WT
KI
thymus
pancreas
lung
ovary
testis
β-actin

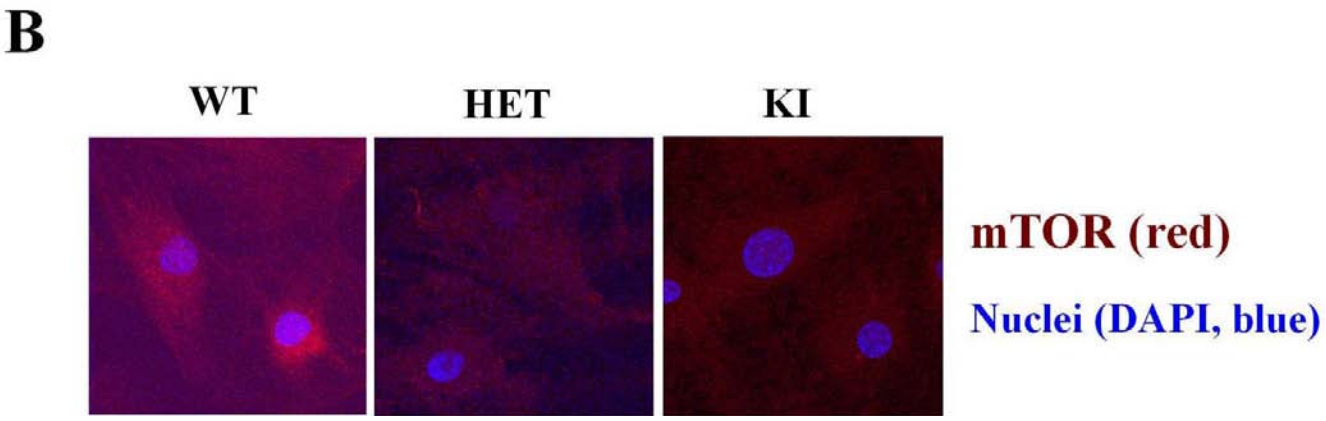
B
WT
HET
KI
mTOR (red)
Nuclei (DAPI, blue)

Figure S3

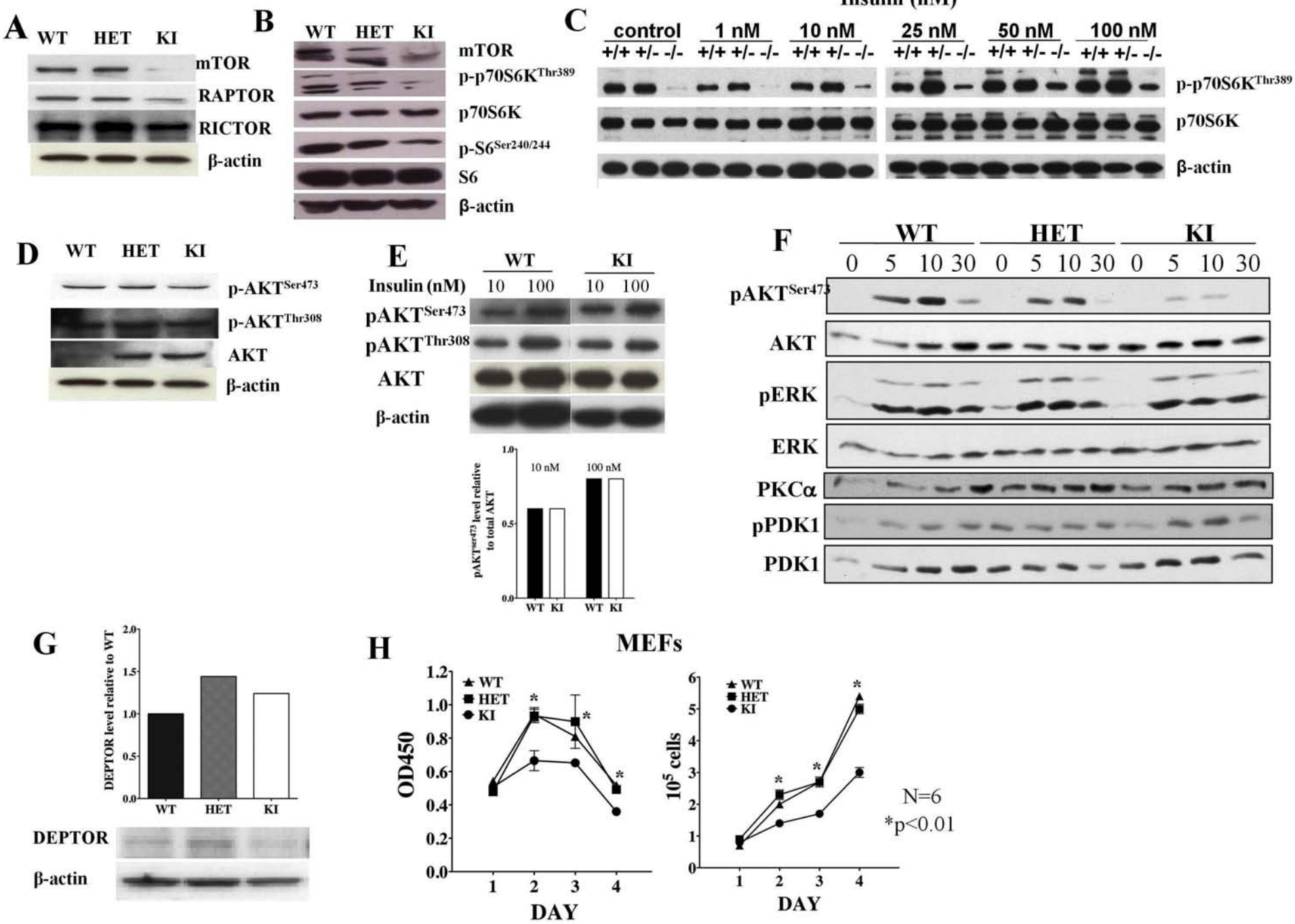
A
WT HET KI
mTOR
RAPTOR
RICTOR
β-actin
B
WT HET KI
mTOR
p-p70S6K^Thr389
p70S6K
p-S6^Ser240/244
S6
β-actin
C
Insulin (nM)
control 1 nM 10 nM 25 nM 50 nM 100 nM
+/+ +/- -/-
p-p70S6K^Thr389
p70S6K
β-actin
D
WT HET KI
p-AKT^Ser473
p-AKT^Thr308
AKT
β-actin
E
WT KI
Insulin (nM) 10 100 10 100
pAKT^Ser473
pAKT^Thr308
AKT
β-actin
pAKT^ser473 level relative to total AKT
10 nM 100 nM
WT KI WT KI
F
WT HET KI
0 5 10 30 0 5 10 30 0 5 10 30
pAKT^Ser473
AKT
pERK
ERK
PKCα
pPDK1
PDK1
G
DEPTOR level relative to WT
WT HET KI
DEPTOR
β-actin
H
MEFs
WT
HET
KI
OD450
DAY
10^5 cells
DAY
N=6
*p<0.01

Figure S4

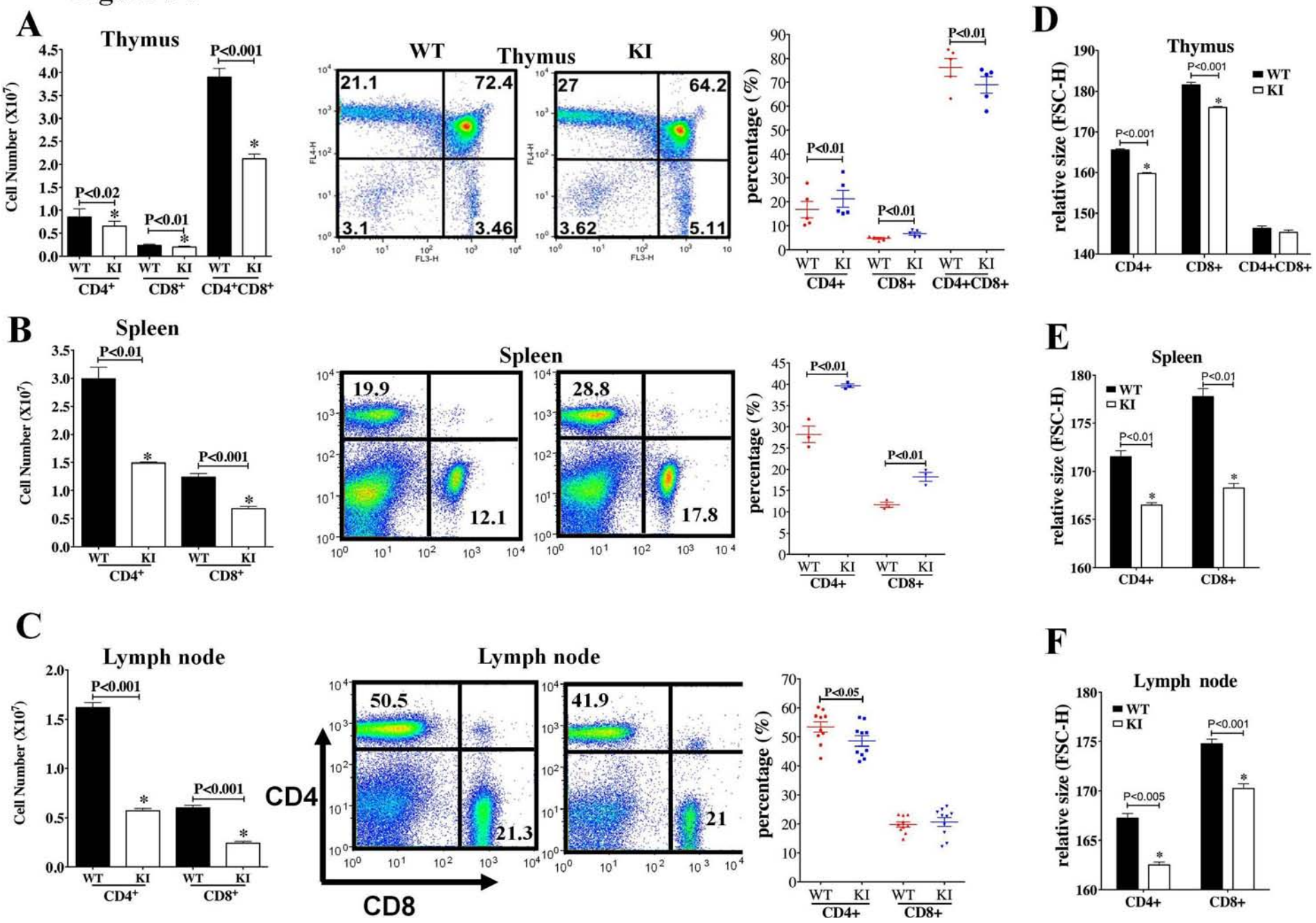
A
Thymus
Cell Number (X10⁷)
P<0.02
P<0.01
P<0.001
WT KI WT KI WT KI
CD4+ CD8+ CD4+CD8+
WT Thymus KI
21.1
72.4
3.1
3.46
27
64.2
3.62
5.11
FL4-H
FL3-H
percentage (%)
P<0.01
P<0.01
P<0.01
WT KI WT KI WT KI
CD4+ CD8+ CD4+CD8+
D
Thymus
relative size (FSC-H)
P<0.001
P<0.001
WT
KI
CD4+ CD8+ CD4+CD8+
B
Spleen
Cell Number (X10⁷)
P<0.01
P<0.001
WT KI WT KI
CD4+ CD8+
Spleen
19.9
12.1
28.8
17.8
percentage (%)
P<0.01
P<0.01
WT KI WT KI
CD4+ CD8+
E
Spleen
relative size (FSC-H)
WT
KI
P<0.01
P<0.01
CD4+ CD8+
C
Lymph node
Cell Number (X10⁷)
P<0.001
P<0.001
WT KI WT KI
CD4+ CD8+
Lymph node
50.5
21.3
41.9
21
CD4
CD8
percentage (%)
P<0.05
WT KI WT KI
CD4+ CD8+
F
Lymph node
relative size (FSC-H)
WT
KI
P<0.005
P<0.001
CD4+ CD8+

Figure S5

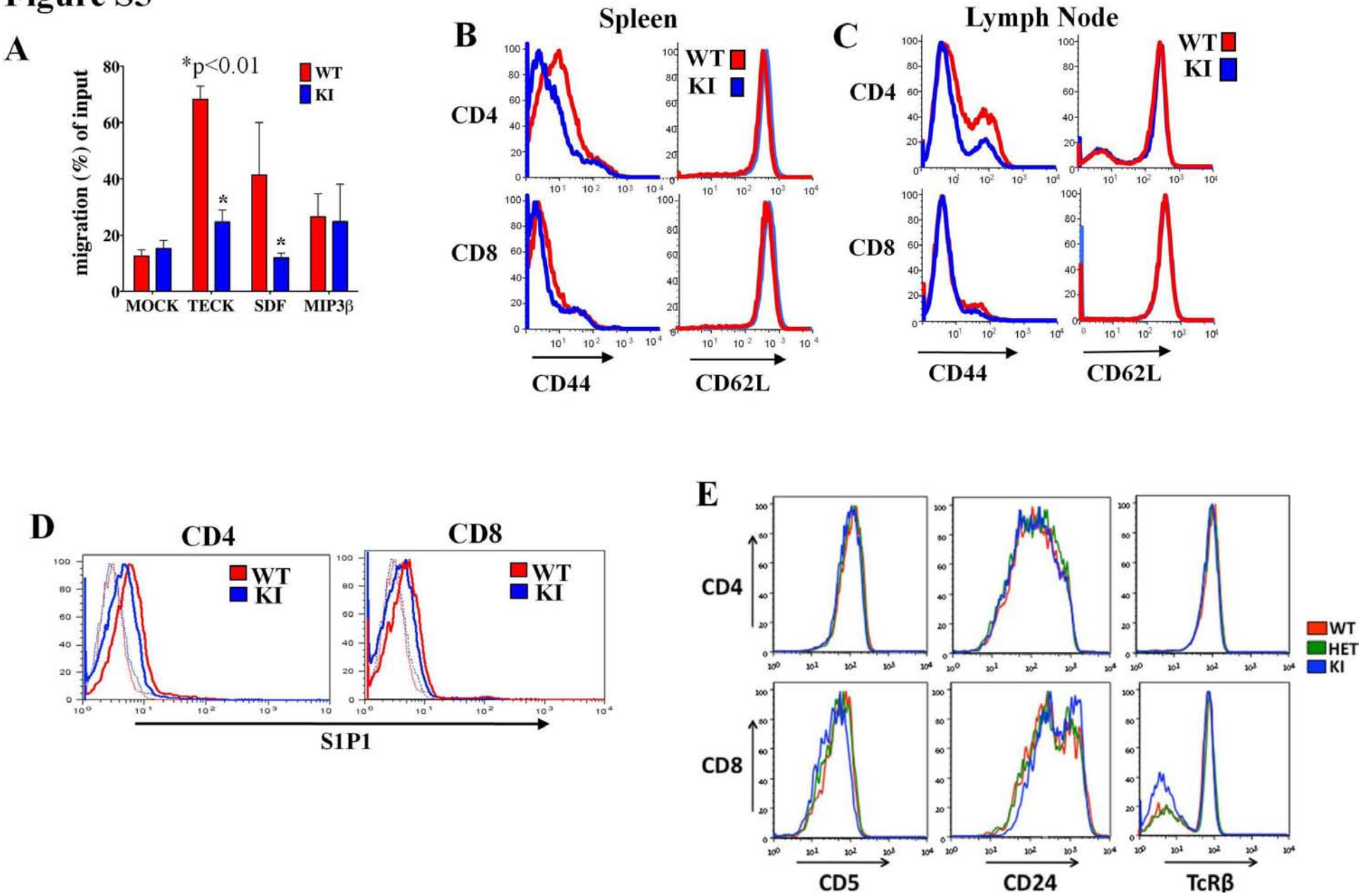
A
*p<0.01
WT
KI
migration (%) of input
MOCK
TECK
SDF
MIP3β
B
Spleen
CD4
CD8
CD44
CD62L
C
Lymph Node
D
CD4
CD8
S1P1
E
HET
CD5
CD24
TcRβ

Figure S6

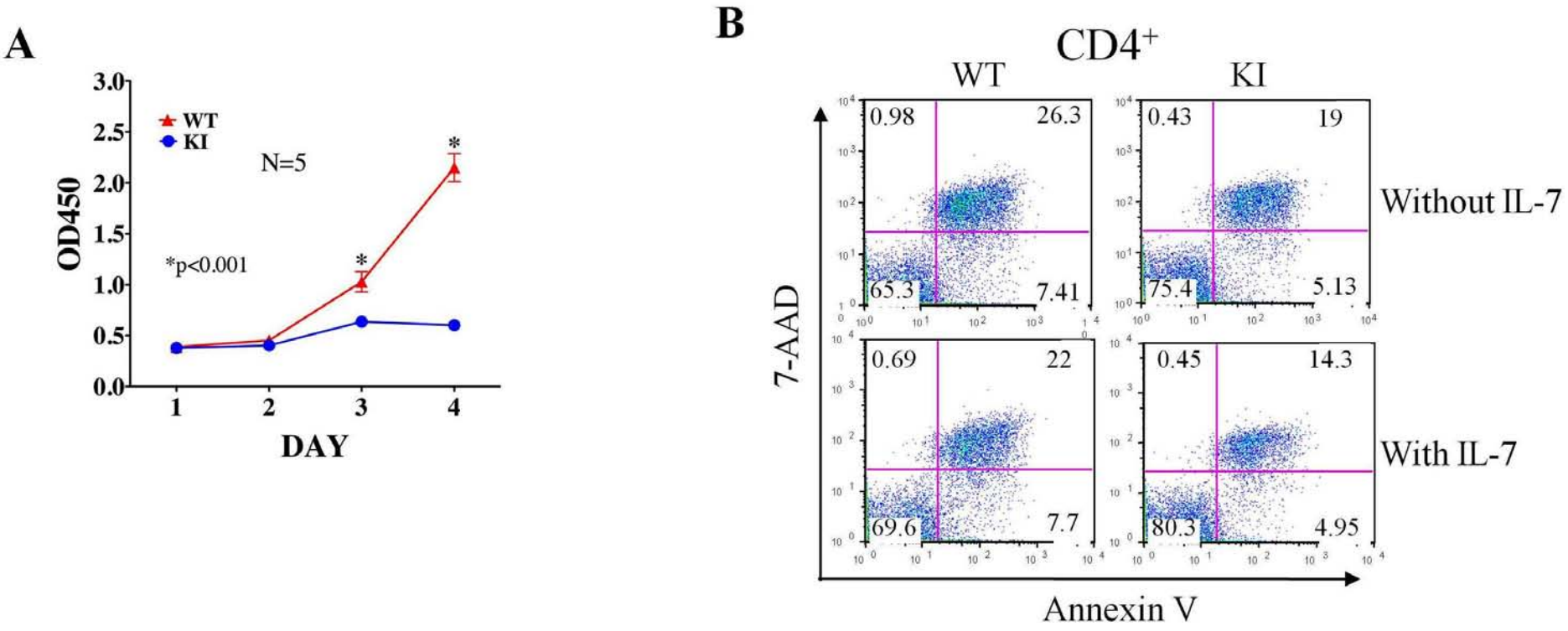
A
WT
KI
N=5
*p<0.001
OD450
DAY
B
CD4+
WT
KI
0.98
26.3
65.3
7.41
0.43
19
75.4
5.13
Without IL-7
0.69
22
69.6
7.7
0.45
14.3
80.3
4.95
With IL-7
7-AAD
Annexin V

Figure S7

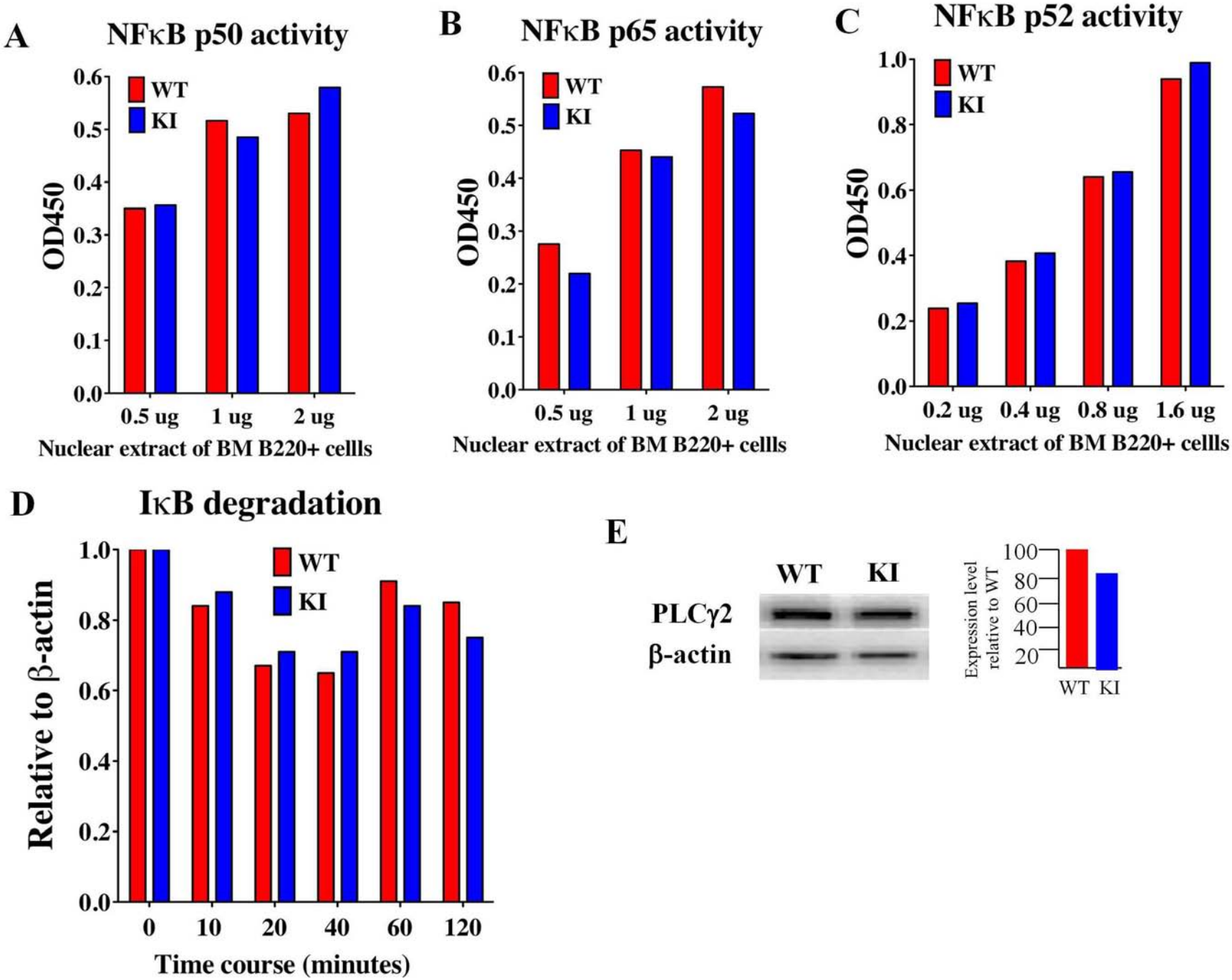
A
NFκB p50 activity
OD450
WT
KI
0.5 ug
1 ug
2 ug
Nuclear extract of BM B220+ cellls
B
NFκB p65 activity
OD450
WT
KI
0.5 ug
1 ug
2 ug
Nuclear extract of BM B220+ cellls
C
NFκB p52 activity
OD450
WT
KI
0.2 ug
0.4 ug
0.8 ug
1.6 ug
Nuclear extract of BM B220+ cellls
D
IκB degradation
Relative to β-actin
WT
KI
0
10
20
40
60
120
Time course (minutes)
E
WT
KI
PLCγ2
β-actin
Expression level relative to WT
WT
KI

Figure S8

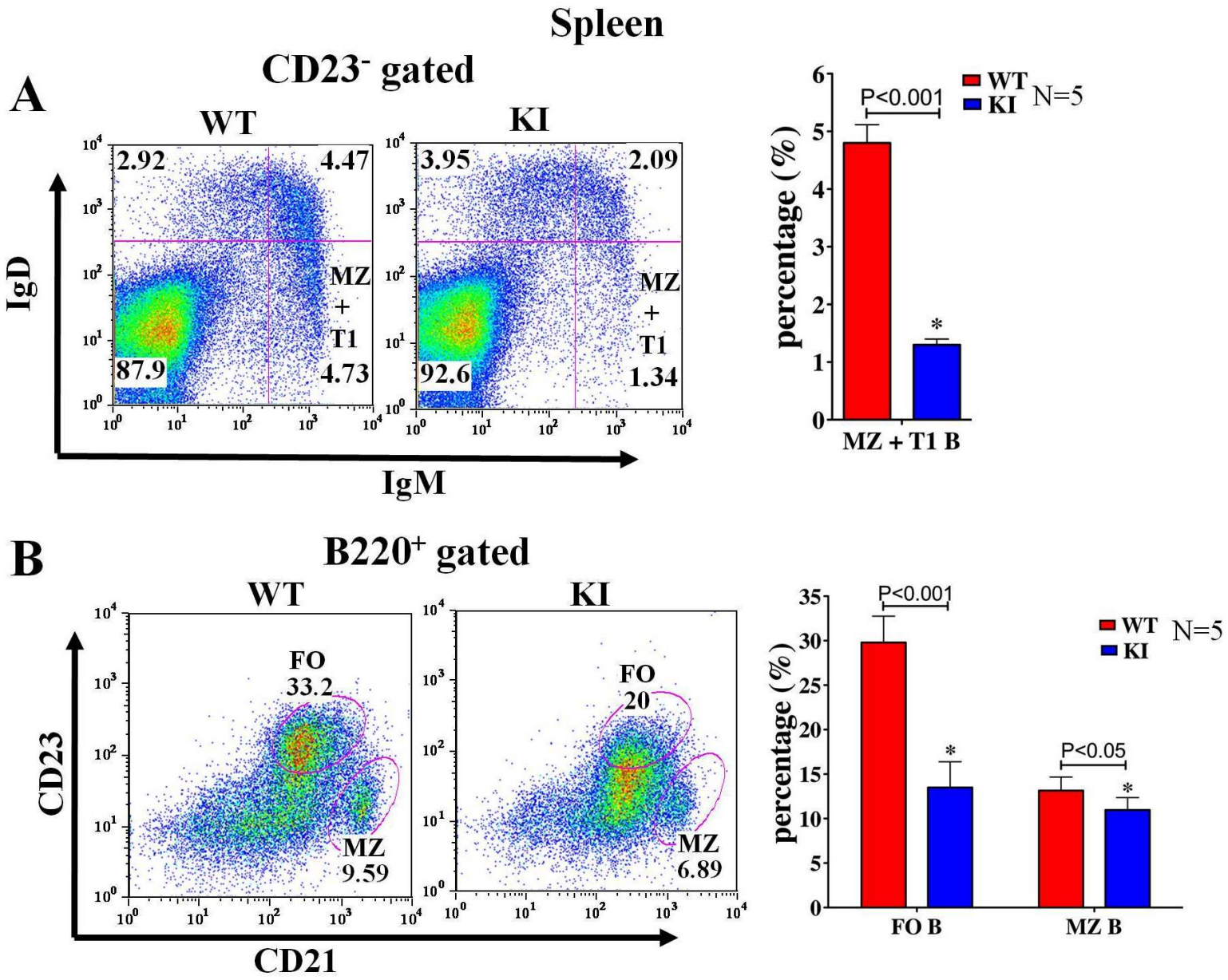
Spleen
A
CD23- gated
WT
KI
IgD
IgM
2.92
4.47
MZ + T1
4.73
87.9
3.95
2.09
MZ + T1
1.34
92.6
P<0.001
WT
KI
N=5
percentage (%)
MZ + T1 B
B
B220+ gated
WT
KI
CD23
CD21
FO
33.2
MZ
9.59
FO
20
MZ
6.89
P<0.001
P<0.05
WT
KI
N=5
percentage (%)
FO B
MZ B

Figure S9

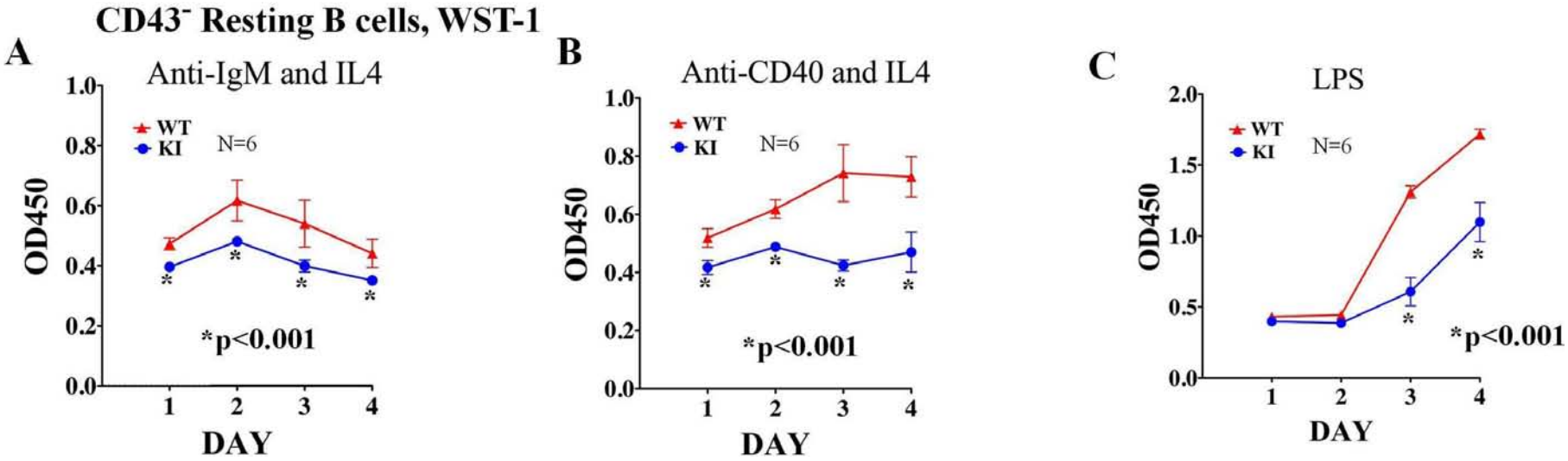
CD43- Resting B cells, WST-1
A
Anti-IgM and IL4
WT
KI
N=6
OD450
DAY
*p<0.001
B
Anti-CD40 and IL4
WT
KI
N=6
OD450
DAY
*p<0.001
C
LPS
WT
KI
N=6
OD450
DAY
*p<0.001

Figure S10

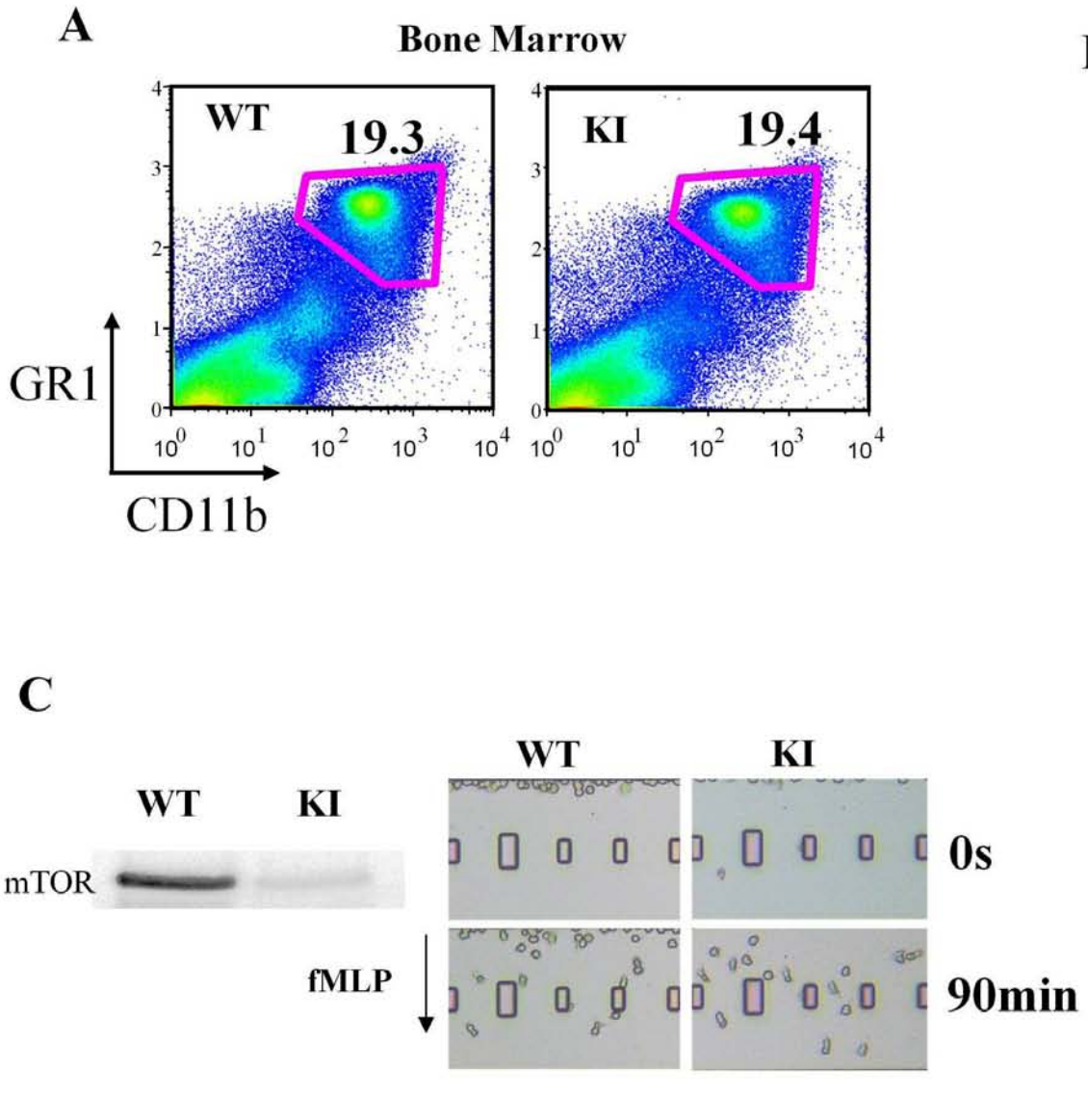
A
Bone Marrow
WT
19.3
KI
19.4
GR1
CD11b
B
Spleen
WT
KI
P<0.008
P<0.02
Percentage (%)
Mac1+
Gr1+
C
WT
KI
mTOR
WT
KI
0s
fMLP
90min
WT
KI
Position from Track Start (um)
Position from Track Start (um)

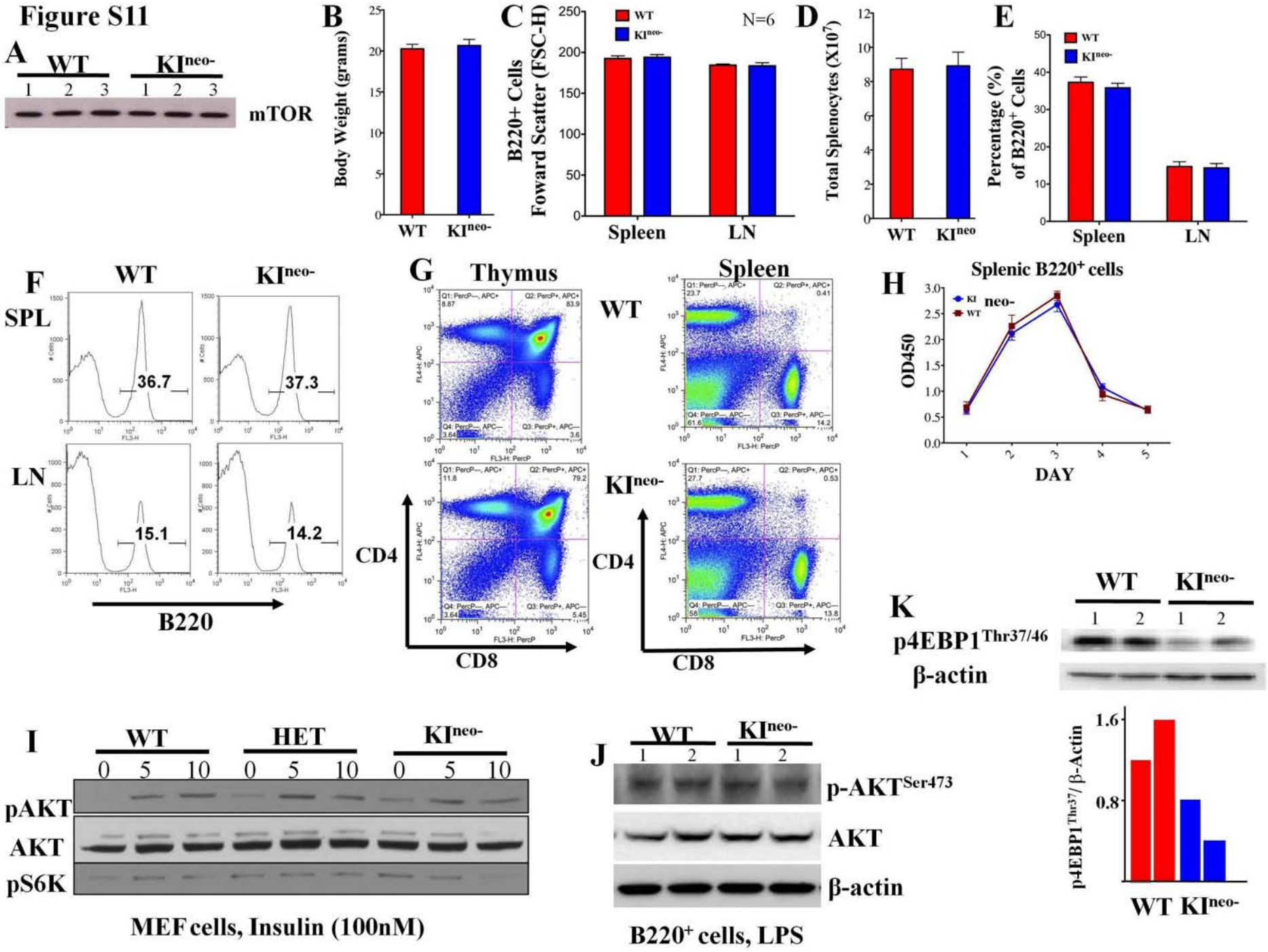
Figure S11
A
WT
KIneo-
1 2 3 1 2 3
mTOR
B
Body Weight (grams)
WT
KIneo-
C
B220+ Cells
Foward Scatter (FSC-H)
WT
KIneo-
N=6
Spleen
LN
D
Total Splenocytes (X10^7)
WT
KIneo
E
Percentage (%) of B220+ Cells
WT
KIneo-
Spleen
LN
F
WT
KIneo-
SPL
LN
36.7
37.3
15.1
14.2
B220
G
Thymus
Spleen
WT
KIneo-
CD4
CD8
H
Splenic B220+ cells
KIneo-
WT
OD450
DAY
I
WT
HET
KIneo-
0 5 10 0 5 10 0 5 10
pAKT
AKT
pS6K
MEF cells, Insulin (100nM)
J
WT
KIneo-
1 2 1 2
p-AKTSer473
AKT
β-actin
B220+ cells, LPS
K
WT
KIneo-
1 2 1 2
p4EBP1Thr37/46
β-actin
p4EBP1Thr37/ β-Actin
1.6
0.8
WT KIneo-